An analysis of the lamellar structure of sea urchin egg cortical granules using X-ray scattering

T. Whalley[a,*], J.G. Grossmann[b], T.J. Wess[a,1]

[a] Centre for Extracellular Matrix Biology, Institute of Biological Sciences, University of Stirling, Stirling FK9 4LA, UK
[b] CLRC Daresbury Laboratory, Daresbury, Warrington WA4 4AD, UK

Abstract Cortical granules (CGs) are secretory vesicles associated with egg and oocyte plasma membranes that undergo exocytosis at fertilisation. In the sea urchin *Strongylocentrotus purpuratus*, the internal organisation of these CGs exhibits a lamellar-type morphology. The different lamellar layers correspond to proteoglycans, structural proteins and enzymes required for fertilisation envelope assembly and modification of the post-fertilisation egg surface. We have studied the lamellar structure of CGs using X-ray scattering and reveal the contrast density variation of the lamellae in the native state. The structure of functionally competent CGs in situ differs significantly from that determined by electron microscopic studies. We observed a strong periodicity of the lamellar structure of 280 Å as opposed to the 590 Å repeat observed previously. Fusion of the CGs produced a loss of the lamellar repeat and the development of a broad peak corresponding to a 20 Å periodicity that may be indicative of the molecular packing in the resulting hydrated gel structure. © 2000 Federation of European Biochemical Societies. Published by Elsevier Science B.V. All rights reserved.

Key words: Cortical granule; Molecular packing; Proteoglycan

1. Introduction

Cortical granules (CGs) are secretory vesicles that are produced during oogenesis. In sea urchins, they form as small vesicles that later fuse to form large, mature CGs that are distributed throughout the cytoplasm [1]. During the completion of oocyte maturation, the CGs migrate to the cell surface and dock with the plasma membrane [2]. At fertilisation, an increase in intracellular Ca^{2+} triggered by gamete interactions leads to CG exocytosis [3,4]. This exocytosis releases structural proteins and proteoglycans that form the fertilisation envelope [5–8], enzymes that modify the egg plasma membrane and are involved in formation and stabilisation of the fertilisation envelope [9–11] and hyalin [12] that is required for blastomer adhesion and cell movements during gastrulation.

In eggs of the sea urchin *Strongylocentrotus purpuratus*, electron microscopic studies have shown that the CG contents are compartmentalised and are arranged into a region of spiral lamellae containing fertilisation envelope proteins, enzymes and highly negatively charged mucopolysaccharides

and a non-lamellar region which contains the protein hyalin [6]. These components are tightly packed and CGs are unusually protein-rich. On exocytosis, the CG contents are released rapidly and the tightly packed proteins and mucopolysaccharides undergo decondensation. Hyalin self-assembles in the presence of millimolar Ca^{2+} to form a stable gel that associates with the surface of the egg [13] whereas the mucopolysaccharides undergo a rapid increase in size that is driven by the release of charged counter-ions and the hydration of multiple sulphate and carboxyl groups [14]. The molecular interactions responsible for stabilising the hydrated structures are unresolved.

Structural studies of CGs have relied on observations made by electron microscopy of fixed, stained specimens. This carries the inherent possibility of artifactual evidence being extrapolated into structural information. It is well established that fixatives such as glutaraldehyde do not fix all types of biological material with equal efficacy. In experiments with sea urchin eggs, it has been shown that different membrane structures are found in samples fixed with glutaraldehyde as opposed to quick frozen specimens [15]. In studies where the lamellar structure of the CGs has been described, samples have been dehydrated, fixed and stained, and the variation in the electron density of CGs has only been implicated by an analysis of electron micrographs of these stained and fixed samples. The sectioning of spherical organelles also leads to inherent problems in the analysis of CG morphology, since the level of sectioning through CGs will produce different frusta of the sphere observed in projection.

In order to understand the functionality of the CGs and their contents, the ultrastructure must also be understood. However, the packing in secretory vesicles of molecules that are usually present in the extracellular matrix as highly hydrated structures such as proteoglycans is a poorly studied area. The questions that have not been possible to address so far relating to the ultrastructure of the condensed dehydrated CG contents include: what is the packing density? What is the average lamellar periodicity? Does this relate to the size of molecular structures and how does this relate to the structure of CG contents following fusion and release? X-ray scattering using synchrotron radiation is capable of probing the internal organisation of the CGs and the inherent nature of this technique gives a result that is the average parameters of many thousands of these organelles. By analysis of the scattering parameters obtained from CG samples, it is possible to determine important features such as the average lamellar spacing, the size of the different phases and the nature of the interface between the contrasting regions of the repeat and their relative density. Such methods have also been success-

*Corresponding author. Fax: (44)-1786-464994.
E-mail: tdw1@stir.ac.uk

[1] Also corresponding author. Fax: (44)-1786-464994; E-mail: tjw3@stir.ac.uk.

fully applied to other spheroid lamellar structures such as starch granules [16] and the analysis of lamellar structures is a key part of polymer technology development [17]. Here we report an X-ray scattering study of CGs in a state that is as close to the native state as possible. The effects of fusion on the structure of the CG contents were also observed on the same samples and allow the dynamic change of loss of lamellar structure with sample hydration to be observed in a single sample.

2. Materials and methods

2.1. Obtaining and handling eggs

Sea urchins of the species *S. purpuratus* were purchased from West-Wind SeaLab Supplies (Victoria, Canada), and were maintained in aquaria in sea water at a temperature of 11°C. Gametes were obtained by injecting 0.5 M KCl into the intra-coelomic cavity of the sea urchins. Eggs were collected into filtered sea water and were maintained on ice until use. Sperm were collected 'dry' and retained refrigerated until use. Fertilisation was assessed microscopically and batches of eggs exhibiting less that 98% fertilisation were discarded.

2.2. Preparation of cell surface complexes (CSCs) and CGs

CSCs were prepared as described previously [18]. Eggs had their jelly coats removed by passing through 90 μm nylon mesh. They were washed three times in artificial sea water and suspended in intracellular medium (IM: 220 mM potassium glutamate, 500 mM glycine, 10 mM NaCl, 5 mM MgCl$_2$, 10 mM ethylene glycol-bis(β-aminoethyl ether)-N,N,N',N'-tetra-acetic acid (EGTA), 1 mM benzamidine HCl, 2.5 mM MgATP, 5 mM dithiothreitol (DTT), 10 μg/ml aprotinin, 10 μg/ml pepstatin, 20 μg/ml leupeptin, pH 6.8). The eggs were washed three times with IM and were transferred to a Potter homogeniser. CSCs were prepared by homogenising the eggs with five or six strokes of a tight-fitting Teflon pestle. After homogenisation, CSCs were pelleted at 700×g for 1 min and suspended in fresh IM. Centrifugation was repeated until the preparation appeared free of contamination and consisted only of large sheets of egg cortex with no intact eggs remaining.

CGs were prepared by a variation of the method of Crabb and Jackson [19]. CSCs were transferred to a high pH CG buffer containing 450 mM KCl, 10 mM EGTA, 50 mM NH$_4$Cl, 1 mM benzamidine HCl, 5 mM DTT, 10 μg/ml aprotinin, 10 μg/ml pepstatin, 20 μg/ml leupeptin pH 9.1 and were incubated for 1 h on ice. During this period, many CGs detached from the plasma membrane. The suspension was centrifuged at 700×g for 1 min at 4°C to remove any large fragments of plasma membrane and CG aggregates. This centrifugation step was repeated twice. Finally, the CGs were collected by centrifugation at 2000×g for 10 min at 4°C and suspended in high pH CG buffer. Prior to use, the pH was adjusted to 6.8 by the addition of 1 M PIPES, pH 6.0. In order to trigger CG fusion, IM containing 5 mM [Ca^{2+}]$_{free}$ was added such that the final [Ca^{2+}]$_{free}$ was ~300 μM.

2.3. Electron microscopy

Purified CGs were fixed in a buffer consisting of 50 mM PIPES, 425 mM KCl, 10 mM MgCl$_2$, 5 mM EGTA, pH 6.8 containing 3% glutaraldehyde for 1 h at 20°C followed by incubation overnight at 4°C. They were centrifuged at 2000×g for 10 min, washed in phosphate buffer pH 7.0 and post-fixed in 1% osmium tetroxide in pH 7.0 phosphate buffer. CGs were centrifuged at 1000×g for 5 min, washed in distilled water and stained with saturated uranyl acetate for 15 min. The samples were dehydrated in a graded acetone series, embedded in Spurrs resin and cured for 48 h at 60°C. Thin sections were cut and were stained with saturated uranyl acetate and Reynold's lead citrate. Specimens were examined using a Philips 301 transmission electron microscope running at 80 kV.

2.4. X-ray scattering

X-ray scattering experiments were conducted at beamline 2.1 of the CLRC Daresbury Synchrotron Radiation Source [20] which provides an excellent optical arrangement for small angle scattering experiments. A suspension of CGs was placed in a sample cell between two thin (20 μm) mica windows. The scattering profile was obtained with a 9.5, 2.5 and 1.25 m camera (i.e. the distance between the sample cell and detector) using a variety of samples prepared in an identical manner. This allowed a large range of reciprocal space to be observed covering a resolution limit of 1/1800 Å to 1/10 Å. The beamsize was 0.8×3 mm and the wavelength 1.54 Å. Data were collected on a gas-filled detector [21] in 1 min time frames that were summed to produce the resultant scattering profiles. Sample blanks containing only buffer in an identical sample cell and detector response measurements were also made. The flux of X-rays at the detector was determined using a pinhole photodiode inside the backstop.

2.5. Data analysis

The two-dimensional scattering profiles obtained from CGs were corrected for the detector efficiency and the background scattering from buffer was subtracted after scaling to correct for differences in transmission. The resultant profiles were then converted into one-dimensional (1D) scattering profiles where each pixel of the detector was converted into its radial and angular co-ordinate and the data projected as a radial function.

The analysis of the data was performed using the program 'Corfunc', a part of the CCP13 suite (Collaborative Computing Project in Fibre Diffraction in the UK, www.dl.ac.uk/SRS/CCP13) that performs a correlation function of the scattering profile after extrapolating the data to a scattering origin and to infinite scattering angle. The program extrapolates to zero scattering angle using an approximation developed by Guinier [22] and the tail fitting is performed with a Gaussian extension of a selected region of the data. The resultant scattering profile is then transformed as a continuous Fourier function with resolution limits of 2000 Å to 100 Å. This function was in turn used to produce a real space correlation function containing data about the lamellar morphology.

3. Results

3.1. Electron microscopy

Samples of CGs were examined following glutaraldehyde fixation and staining with uranyl acetate and lead citrate. As has been shown in previous studies, the contents of CGs from *S. purpuratus* are composed of two distinct regions (Fig. 1). The first is an amorphous region that is thought to contain hyalin [12]. The second region has a characteristic lamellar appearance with alternating bands of contrasting electron
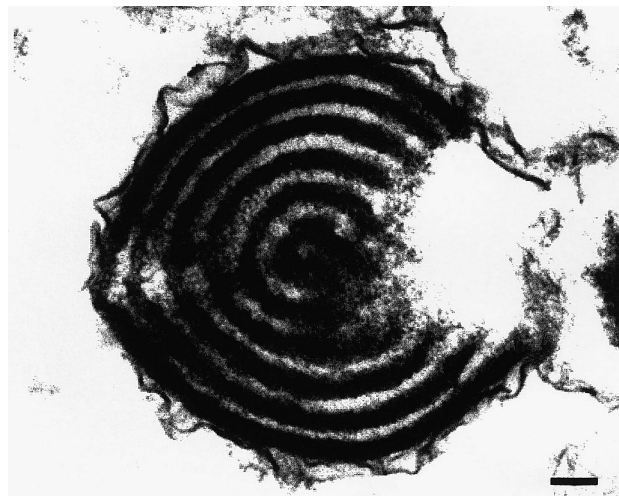

Fig. 1. Electron micrograph of a CG. The electron-dense and electron-lucent lamellae are visible in CGs fixed and stained with uranyl acetate and lead citrate. The unstained region is thought to consist primarily of hyalin. The thicknesses of the electron-dense and electron-lucent lamellae are approximately equal. Some fine structure can be observed in the electron-lucent region. Scale bar is 1000 Å.

density that are thought to contain distinct macromolecular components [23,24]. An analysis of these lamellae shows that the periodicity between the centres of adjacent electron-dense bands is 590 ± 40 Å.

3.2. X-ray scattering

An initial inspection of the X-ray scattering profile (Fig. 2) immediately indicates that the lamellar morphology apparent in Fig. 1 has sufficient regularity to produce a diffraction peak. However, the coherence of the structure only leads to a single observable peak; this is common in most lamellar structures. The periodicity of the peak observed using the 9.5 m camera corresponds to a periodicity of 300 Å, this is more rigorously defined in the correlation function analysis as a value of 280 Å. This value is in contrast to the periodicity observed in Fig. 1 and other electron microscopy studies where the spacing of the observed lamellae is close to twice this value. Close examination of the X-ray intensity profile does not show any corresponding peak in the region of ~600 Å (this position is indicated in Fig. 2) although the first order of collagen could be resolved clearly (670 Å). A correlation function analysis takes the diffraction data and converts the scattering profile via a Fourier analysis into a real space representation of the periodicity within the scattering objects. Since each scattering object (CG) is isotropically disorientated, we can only obtain the distances between phases of the lamellae and an electron density profile can only be inferred. The correlation function analysis allows us to obtain information on the electron density between the repeating structures and also the relative lengths of the different contrasting regions. Fig. 3 shows the correlation function. The correlation consists of three major components, the slope of the initial linear region (close to the origin), the first minimum of the 1D correlation function and the first maximum of

Fig. 3. The correlation function derived from the intact CG scattering profile. The correlation function from intact CGs was determined using the 'Corfunc' programme of the CCP13 suite. The *x* axis corresponds to the spacing in Å. The *y* axis designates γ, the correlation function. The lamellar period corresponds to the spacing of the first maximum (280 Å). The thickness of the dense region is obtained by extrapolating the slope of the first linear portion of the correlation function to where it corresponds to the γ value of the first minimum and the value is read from the *x* axis. This construct is indicated by the dotted lines. The value obtained from this is 90 Å and implicitly, the less dense region has a length of 190 Å.

the 1D correlation function. From these values, we obtained data for the length of the average lamellar periodicity and the relative size of the two components that make up the lamellae (dense and soft regions). Due to Babinet's principle, the dense and soft regions of the lamellar structure cannot be defined unambiguously (i.e. the structure could be inverted). If the dense region corresponds to the 90 Å periodicity, then the less dense region corresponds to an 190 Å periodicity (see Fig. 5). The regularity of the bands is only sufficient to pro-
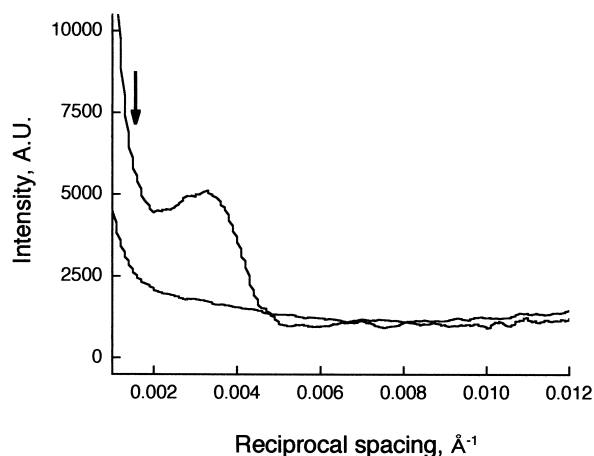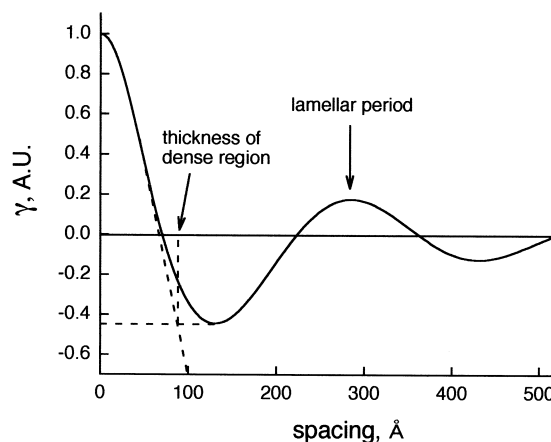

Fig. 2. Scattering profiles of CGs with a 9.5 m camera. The profiles are derived from the radial integration of each two-dimensional scattering pattern after background corrections for the scattering from water and the detector efficiency. A typical profile from the intact CGs is shown. A discrete interference function can be observed corresponding to a spacing of ~300 Å. This appears to be the only interference function visible and is approximately half the periodicity of the repeat observed by electron microscopy. The scattering curve obtained from CGs fused by the addition of Ca^{2+} is shown beneath the intact CG profile and contains no interference maximum. No peak corresponding to the ~590 Å repeat (as observed in the electron microscope) can be seen; the position where this would be expected is marked with an arrow.
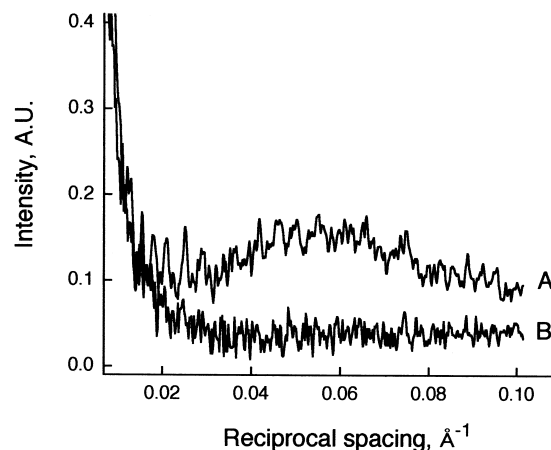

Fig. 4. Scattering profiles of CGs recorded with a 1.25 m camera. This was used to observe the interference profile at higher scattering angles. The profile from fused (and therefore hydrated) CGs (line A) corresponds to the broad maximum corresponding to a periodicity of ~20 Å. This periodicity has not been observed in the electron micrographs of fused CG materials and indicates the potential advantage of an X-ray scattering approach in elucidating true structural alterations during exocytosis of macromolecules. In contrast (line B), the scattering profile from intact CGs does not show this periodicity, indicating that this is a feature developed during hydration of the CG contents following membrane fusion.

duce a single interference peak. Although it is possible to derive other structural parameters from the correlation function, these are probably too speculative since the correlation function does not contain a flat region around the first minima indicating a significant length of polycrystalline material. Deviations from the ideal lamellar organisation that are probably inherent in biological structures can make the interpretation of other parameters unreliable.

The use of shorter camera lengths allowed shorter length scales to be probed in both fused (Ca^{2+}-treated) and intact CGs. A 2.5 m camera did not reveal any further periodic structures, however, the fused CGs did present a broad peak corresponding to a periodicity of approximately 20 Å as observed using a 1.25 m camera (see Fig. 4). This may correspond to a significant periodic structure that comprises the ultrastructure of the expanded proteoglycan or the hyalin layer. The peak was however very broad, corresponding to a wide distribution of periodicity values centred around 200 Å spacing. These results indicate that the small angle scattering process can be used to monitor the dynamic changes in proteoglycan hydration in a time-resolved manner.

4. Discussion

Sea urchin egg CGs represent a novel sub-cellular structure in that they contain a large-scale lamellar structure that consists of condensed proteoglycans and proteins. The condensed (dehydrated) phase of proteoglycans and other secreted macromolecular assemblies is poorly understood and the system described here using small angle X-ray scattering constitutes a physiologically important dynamic process where the condensed phase is converted into a fully hydrated structure. The basis of the lamellar structure as reported by electron microscopy is questioned by the results shown here. All of the transmission electron microscopy studies that we could find involved samples being counter-stained with charged electron-dense materials such as uranyl acetate and lead citrate in addition to post-fixation with osmium tetroxide. Electron microscopy studies of CGs obtained from *S. purpuratus* state that the electron-dense material forms the spiral lamellar structure [23]. Immunoelectron microscopy analyses have indicated that the enzyme ovoperoxidase is located in the electron-dense region where it is co-localised with proteoliaisin [23]. The CG protease responsible for clipping the vitelline posts and degrading the plasma membrane sperm receptor is also localised to the electron-dense region of the CGs [25]. There is less evidence concerning the nature of the less electron-dense regions of the CGs but it is likely that these regions contain some protein components together with the bulk of the mucopolysaccharides.

The difference between the observed periodicity of the CGs in the native state by X-ray scattering and the stained, fixed samples observed by electron microscopy may be due to the staining procedures that produce contrasting density in electron microscopy. The residual stain that produced the dark layer of the spiral structure may result from two effects. Firstly, the stain may occupy a region of lower density, i.e. positive staining, or secondly, the net charge of the different layers may lead to differential labelling. In electron microscopy, the thicknesses of the two phases are comparable; if this repeat were to provide the major step function that caused the diffraction observed in small angle scattering, a prominent

diffraction peak should be observed corresponding to a periodicity of ~590 Å. A well-ordered step function with contrasting regions of equal thickness should conversely provide a diffraction series where the odd orders are strong; this does not correlate well with the diffraction data where the periodicity would correspond to the second order of a 590 Å repeat. Furthermore, strong secondary maxima are rarely observed in the scattering of long-range lamellar structures. A plausible explanation is that a strong periodic function within the contents of CGs corresponds to the interface between the two regions and is a pseudo-periodic structure of the longer range periodicity generated by differential staining observed in the electron microscope. This effect dominates the periodicity

a) Electron density step function as observed in TEM

b) Inferred electron density profile from TEM

590 Å

c) Electron density profile estimated by X-ray scattering of native unstained samples
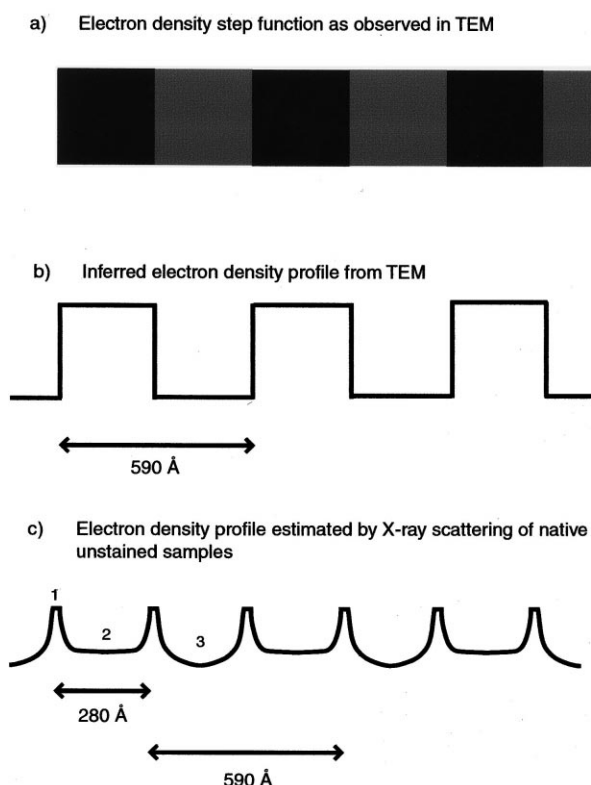
1
2
3

280 Å

590 Å

Fig. 5. Interpretation of the electron density profile. An idealised portion of the spiral lamellar structure representative of what is seen in the electron microscope is shown in part a. This consists of alternate blocks of identical size with contrasting density produced by staining with electron-dense stains. The corresponding electron density profile is shown in part b with the length of the lamellar repeat identified. In part c, we show the lamellar repeat as suggested by the X-ray scattering studies presented here. A 280 Å repeat is the most prominent feature, however, this is a pseudo-period since the dense regions defined by the correlation function are the boundaries between the dense and electron-lucent regions observed in the electron microscope. Region 1 corresponds to the electron-dense boundary; this is the dense region as defined by the correlation function. Region 2 corresponds to the part of the CGs that is protein-rich and region three represents the electron-lucent part of the CGs that is rich in mucopolysaccharides; these correspond to the less dense region as described by the correlation function. In this model density profile, the true fundamental periodicity is close to 590 Å. However, it is of insufficient contrast when compared with the pseudo-periodic electron density contrast. We envisage that the differential staining observed in electron microscopy is due to different molecular densities that are bounded by these sharp interfaces. This model therefore reconciles the scattering data and electron microscope observations.

observed in X-ray scattering of CGs in the native state. An interpretation of the differences is shown in Fig. 5.

It is of interest to note that a rotary shadowing electron microscopy study of etched sections of CGs also reveals the lamellar structure, with the additional feature of a differential density within the lamellar repeat [6]. It may be the case that this feature is even more prominent within the intact structure. Such a structural feature may provide an indication as to how CGs are formed; a region of higher electron density between the principal electron-dense and -lucent regions will provide an effective barrier to the mixing of components prior to exocytotic release from the egg. This is clearly important as cross-linking between the components post-exocytosis is important in stabilising the fertilisation envelope and must not occur prior to content hydration and expansion. When precocious cross-linking occurs, exocytosis takes place at fertilisation but CG expansion and the formation of the fertilisation envelope is prevented [26].

The approach described here could also prove useful in elucidating the structures of other non-fixed secretory vesicles or organelles and the dynamic changes that can occur on native samples. The use of the correlation function program also provides a benchmark method for the analysis of biological lamellar samples and allows a rigorous analysis of the data without the subjectivity that can result from electron microscopy. This approach may also permit a determination of the mechanisms by which extracellular matrix components are assembled following exocytosis from cells.

References

[1] Anderson, E. (1968) J. Cell Biol. 37, 514–539.
[2] Laidlaw, M. and Wessel, G.M. (1994) Development 120, 1325–1333.
[3] Steinhardt, R.A., Zucker, R. and Schatten, G. (1977) Dev. Biol. 58, 185–196.
[4] Swann, K. and Whitaker, M.J. (1986) J. Cell Biol. 103, 2333–2342.
[5] Chandler, D.E. (1991) J. Electron. Microsc. Tech. 17, 266–293.
[6] Larabell, C. and Chandler, D.E. (1991) J. Electron. Microsc. Tech. 17, 294–318.
[7] Detering, N.K., Decker, G.L., Schnell, E.D. and Lennarz, W.D. (1977) J. Cell Biol. 75, 899–914.
[8] Baginski, R.M., McBlaine, P.J. and Carroll, E.J. (1982) Gamete Res. 6, 39–52.
[9] Schuel, H., Wilson, W.L., Chen, K. and Lorand, L. (1973) Dev. Biol. 34, 175–186.
[10] Kay, E.S. and Shapiro, B.M. (1987) Dev. Biol. 121, 325–334.
[11] Moy, G.W., Kopf, G.S., Gache, C. and Vacquier, V.D. (1983) Dev. Biol. 100, 267–274.
[12] Hylander, B.L. and Summers, R.C. (1982) Dev. Biol. 93, 368–380.
[13] Chandler, D.E. and Heuser, J. (1981) Dev. Biol. 82, 393–400.
[14] Schuel, H., Kelly, J.W., Berger, E.R. and Wilson, W.L. (1974) Exp. Cell Res. 88, 24–30.
[15] Chandler, D.E. (1984) J. Cell Sci. 72, 23–36.
[16] Waigh, T.A., Donald, A.M., Heidelbach, F., Riekel, C. and Gidley, M.J. (1999) Biopolymers 49, 91–105.
[17] Polis, D.L., Winey, K.I., Ryan, A.J. and Smith, S.D. (1999) Phys. Rev. Lett. 83, 2861–2864.
[18] Whalley, T. and Sokoloff, A. (1994) Biochem. J. 302, 391–396.
[19] Crabb, J.H. and Jackson, R.C. (1985) J. Cell Biol. 101, 2263–2273.
[20] Townes-Andrews, E., Berry, A., Bordas, J., Mant, P.K., Murray, K., Roberts, K., Sumner, I., Worgan, J.S. and Lewis, R. (1989) Rev. Sci. Instrum. 60, 2346–2349.
[21] Lewis, R. (1994) J. Synchrotron Radiat. 1, 43–53.
[22] Guinier, A. and Fournet, G. (1955) Small-Angle Scattering of X-Rays, Wiley, New York.
[23] Somers, C.E., Battaglia, D.E. and Shapiro, B.M. (1989) Dev. Biol. 131, 226–235.
[24] Wessel, G.M. (1989) J. Histochem. Cytochem. 37, 1409–1420.
[25] Alliegro, M.C. and Schuel, H. (1988) Dev. Biol. 125, 168–180.
[26] Whalley, T., Terasaki, M., Cho, M.-S. and Vogel, S.S. (1995) J. Cell Biol. 131, 1183–1192.